

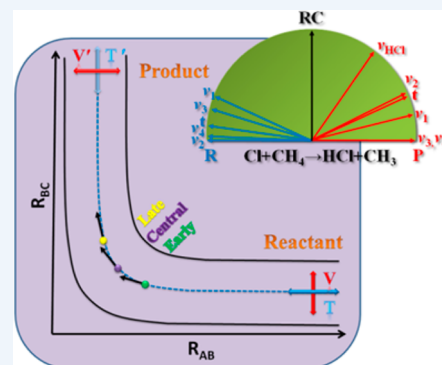
The Sudden Vector Projection Model for Reactivity: Mode Specificity and Bond Selectivity Made Simple

Hua Guo* and Bin Jiang

Department of Chemistry and Chemical Biology, University of New Mexico, Albuquerque, New Mexico 87131, United States

CONSPECTUS: Mode specificity is defined by the differences in reactivity due to excitations in various reactant modes, while bond selectivity refers to selective bond breaking in a reaction. These phenomena not only shed light on reaction dynamics but also open the door for laser control of reactions. The existence of mode specificity and bond selectivity in a reaction indicates that not all forms of energy are equivalent in promoting the reactivity, thus defying a statistical treatment. They also allow the enhancement of reactivity and control product branching ratio. As a result, they are of central importance in chemistry.

This Account discusses recent advances in our understanding of these nonstatistical phenomena. In particular, the newly proposed sudden vector projection (SVP) model and its applications are reviewed. The SVP model is based on the premise that the collision in many direct reactions is much faster than intramolecular vibrational energy redistribution in the reactants. In such a sudden limit, the coupling of a reactant mode with the reaction coordinate at the transition state, which dictates its ability to promote the reaction, is approximately quantified by the projection of the former onto the latter. The SVP model can be considered as a generalization of the venerable Polanyi's rules, which are based on the location of the barrier. The SVP model is instead based on properties of the saddle point and as a result capable of treating the translational, rotational, and multiple vibrational modes in reactions involving polyatomic reactants. In case of surface reactions, the involvement of surface atoms can also be examined. Taking advantage of microscopic reversibility, the SVP model has also been used to predict product energy disposal in reactions. This simple yet powerful rule of thumb has been successfully demonstrated in many reactions including uni- and bimolecular reactions in the gas phase and gas–surface reactions. The success of the SVP model underscores the importance of the transition state in controlling mode-specific and bond-selective chemistry.



It has long been recognized that dynamics of many reactions are not statistical, because energy in different forms has different efficacies in promoting the reaction. The manifestation of the nonstatistical nature is mode specificity and related bond selectivity.^{1,2} Mode specificity is defined by the differences in reactivity due to excitations in various reactant modes, while bond selectivity refers to selective bond breaking in a reaction. These phenomena not only shed light on reaction dynamics but also open the door for laser control of reactions.³

Mode specificity and bond selectivity have been widely observed, particularly in reactions in the gas phase.^{4–14} For instance, the groups of Crim and Zare have demonstrated that the reactivity and product distribution can vary significantly for reactions involving H₂O or CH₄ when their normal vibrational modes are excited.^{4–9} Reactions with deuterated reactants showed strong selective bond breaking when local mode vibrations were excited.^{15–19} Mode specificity and bond selectivity have also been observed in unimolecular decomposition.^{20,21} More recently, similar phenomena have been reported for dissociative chemisorption of small molecules on metal surfaces.^{22,23}

Theoretical characterization of mode specific and bond selective chemistry has been quite successful, using either quasi-classical trajectories or wave packets on global potential energy surfaces (PESs).^{24–38} However, it remains unsatisfactory

because such calculations are difficult and costly, especially for polyatomic reactions. It is highly desirable to establish simple rules of thumb without performing elaborate dynamical calculations on multidimensional PESs. In turn, such rules offer insights on fundamental principles governing reaction dynamics.

One such rule of thumb was proposed by John Polanyi several decades ago. Distilled from extensive experimental and theoretical studies of atom–diatom reactions, Polanyi pointed out two limiting scenarios.³⁹ If a reaction has a reactant-like or “early” barrier, translational energy is more effective in overcoming the barrier than vibrational energy. On the other hand, vibrational excitation becomes more effective than translational excitation if the reaction has a product-like or “late” barrier. Over the years, Polanyi's rules have provided valuable guidance in predicting the relative efficacy between the vibrational and translational modes in promoting reactivity. However, these venerable rules are not quantitative and are difficult to extend to reactions involving polyatomic reactants, which have more than one vibrational mode. Neither do they provide any guidance on the efficacy of rotational modes, reactions with a “central” barrier, or bond selectivity.

Received: September 27, 2014

Published: November 13, 2014

Furthermore, some recent studies have questioned the general applicability of these rules in relatively simple reactive systems.^{10,12,29,40,41}

The central questions this Account attempts to address are (1) whether a more general set of rules can be found for predicting at a semiquantitative level mode specificity and bond selectivity in reactions, without doing the costly dynamical calculations; and (2) if so, what would fundamental principles these rules reveal?

We start by considering the time scales of two important events in a bimolecular reaction. The first is for the collision between two reactants, while the other is concerned with the rate of energy flow within the reactants. For an activated reaction with a substantial barrier, the collision time is often very short because the two collisional partners need significant kinetic energy to overcome the barrier. On the other hand, the time needed for intramolecular vibrational energy redistribution⁴² (IVR) within each reactant is often long, particularly for molecules with sparse densities of states. (We emphasize that we are concerned here with IVR within each reactant, rather than that in the activated collision complex, which is of course very fast.) The disparity between these two time scales in a typical bimolecular reaction allows one to consider the reaction within the sudden limit, in which the internal energy distributions in both reactants are maintained until they reach the strongly interacting region of the PES.

Let us now consider the capacity of different reactant modes in promoting such a reaction. To this end, it is helpful to invoke the concept of reaction coordinate (RC), which can be considered as a one-dimensional coordinate connecting reactants to products through the transition state. At the transition state, the RC corresponds to the motion surmounting the saddle point, characterized by a normal mode with an imaginary frequency. In this picture, it becomes apparent that mode specificity is associated with the ability of a reactant mode, whether it is vibration, rotation, or translation, to couple with the RC at the transition state. This of course is not an entirely new idea. To quote Crim in a 2008 review,² “initial excitation of a motion that has a large component along the reaction coordinate should accelerate the reaction”. But how can such a component be evaluated? Some valuable hints are given by Polanyi, who attributed the coupling to the location of the barrier.³⁹

To illustrate this point, the RC vector for a hypothetical atom–diatom reaction is shown in Figure 1 for an “early”,

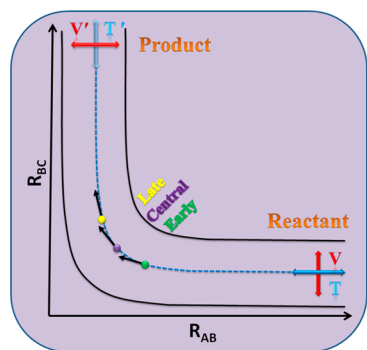


Figure 1. Schematic illustration of the alignment of the reactant and product vibrational (V/V') and translational (T/T') vectors with the reaction coordinate vector at an “early”, “central”, or “late” transition state for a hypothetical atom–diatom reaction $A + BC \rightarrow AB + C$.

“late”, or “central” barrier, along with the vibrational and translational vectors of both the reactants and products. Note that the kinematic factors are not considered in the schematic depiction of the PES. For an early barrier reaction, for example, it is not difficult to see that the translational vector is well aligned with the RC. On the other hand, the reactant vibrational vector has a large component in the RC of a “late” barrier reaction. In other words, the alignment of reactant vectors with the RC at the transition state is correlated to the location of the barrier!

The sudden vector projection (SVP) model⁴³ places a premium on the alignment of a reactant vector with the RC vector at the transition state, rather than the location of the barrier. Within the sudden limit, we argue that the coupling between a reactant mode and the RC is proportional to the alignment of the two vectors, which quantifies its ability to promote the reaction. Indeed, SVP calculations for several prototypical atom–diatom reactions are consistent with Polanyi’s rules.⁴³

By means of microscopic reversibility, the SVP model can also be used to predict energy disposal in the products, which can be considered as mode specificity for the reverse reaction.⁴³ The alignment of the product vectors with the RC vector as shown in Figure 1 suggests that the energy is largely disposed into the translational coordinate in a “late” barrier reaction while the product vibration is likely excited in an “early” barrier reaction, again consistent with Polanyi’s predictions.

At this point, it is worthwhile to provide some details on the implementation of the SVP model.⁴³ The RC vector (\vec{Q}_{RC}) can be readily determined at the saddle point via a normal-mode analysis since it corresponds to the mode traversing the barrier with an imaginary frequency. The determination of reactant mode vectors is more involved and contains some arbitrariness. Our recipe calls for separation of the reactants from the saddle point along the scattering coordinate, with minimal reorientation. The latter is important because it allows the treatment of the translational coordinate, which is isotropic, and internal modes of the reactants, which depend on the orientation, on equal footing. Once the asymptote is reached, the reactants are optimized and the corresponding vectors are obtained via a normal-mode analysis. In addition to the high-frequency vibrational modes ($\vec{Q}_i, i = \nu$), there are also low-frequency modes for the rotational ($\vec{Q}_i, i = r$) and relative translational ($\vec{Q}_i, i = t$) modes. It is important that the Eckart conditions are imposed to remove the six overall translational and rotational degrees of freedom of the reactive system.⁴⁴ This procedure can be readily realized in existing programs such as Polyrate⁴⁵ and Gaussian,⁴⁶ although one should pay attention to mass scaling and normalization in each program. The vector projection is trivial, yielding the SVP values: $\eta_i = \vec{Q}_i \cdot \vec{Q}_{RC} \in [0,1]$. The larger the value, the better alignment with the RC, and thus the larger efficacy for promoting the reaction. We note in passing that the SVP model does not offer any guidance on inhibitory effects, because $\eta_i = 0$ simply indicates no coupling with the RC.

The most important feature of the SVP model is its applicability to reactions involving polyatomic molecules. Unlike atom–diatom reactions where the vector alignment can be readily illustrated in Figure 1, projections for polyatomic reactants are often obscured by high dimensionality. Nonetheless, it is convenient to plot the alignment of both reactant and product vectors with the RC vector, as done in Figure 2 for the $\text{Cl} + \text{CH}_4 \rightarrow \text{CH}_3 + \text{HCl}$ reaction.⁴⁷ Here, it is shown that the two stretching modes of CH_4 (ν_1 and ν_3) are best aligned with

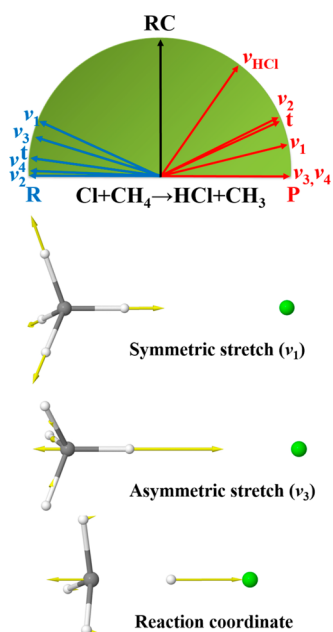


Figure 2. Projections of reactant and product vectors onto the reaction coordinate vector at the transition state for the $\text{Cl} + \text{CH}_4 \rightarrow \text{HCl} + \text{CH}_3$ reaction.⁴⁷ The symmetric and asymmetric stretching, as well as the reaction coordinate vectors are shown.

\vec{Q}_{RC} while the bending (ν_2 and ν_4) and translational (t) modes are less well aligned. Indeed, it is not difficult to visualize the large components of the two stretching modes in the RC vector as shown in Figure 2. It is worth mentioning that the asymmetric stretching mode (ν_3) is 3-fold degenerate, and the SVP value here is averaged over all three vectors. On the product side, HCl is predicted to be vibrationally excited, as does the umbrella vibration of CH_3 (ν_2). These predictions are consistent with the available experimental and theoretical results.⁴⁷

In another example, we have recently demonstrated via full-dimensional quantum dynamical calculations that all vibrational modes of H_2O promote the $\text{F} + \text{H}_2\text{O} \rightarrow \text{HF} + \text{OH}$ reaction more effectively than translation energy.⁴¹ Since this reaction has a definite “early” barrier, this observation is inconsistent with the prediction of Polanyi’s rules. However, our SVP calculations (Figure 3) indicated that the projections of the

reactant vibrational modes are more strongly coupled with \vec{Q}_{RC} than translation, thus providing a rationalization of the surprising results. Also shown in Figure 3 are the SVP values for several similar reactions, and they are also consistent with the quantum cross sections shown in the same figure.

In addition to efficacies of the reactant vibrational and translational modes, the SVP model also offers insights on the effect of reactant rotational excitations.⁴⁸ For the $\text{H} + \text{H}_2$ reaction, the SVP projection for the H_2 rotational mode is zero, because it is orthogonal to the RC at the collinear transition state, as shown in Figure 3. This is consistent with the weak rotational effect in this reaction. However, there are cases where the reactant rotation strongly enhances reactivity.⁴⁸ One example is the $\text{F} + \text{H}_2$ reaction where the transition state is bent and the H_2 rotation has a large component in the RC, as shown in Figure 4, which is evidenced by a large SVP value of 0.64.⁴⁸ It should be noted that predicting efficacies for rotational excitations is less reliable because of complications introduced by angular momentum coupling.

Thus far, the SVP model has been applied to atom–diatom,^{43,48,49} atom–triatom,^{37,48,50} diatom–diatom,⁵¹ atom–tetraatom,⁵² diatom–triatom,^{52,53} diatom–tetraatom,⁵⁴ atom–pentaatom,^{47,55} and diatom–pentaatom reactions,⁵⁶ as well as some unimolecular processes.^{57,58} The predictions are in general accord with experimental and theoretical results. In addition, Bowman and co-workers have proposed a similar model for predicting tunneling rates based on projecting various normal mode vectors onto the RC,^{59–61} which has also shown much promise.

While molecules in these gas phase reactions have relatively sparse densities of state, slow IVR cannot be automatically assumed if a metal surface is involved, because surface phonons and electron–hole pairs allow fast energy dissipation.²² Yet, the SVP model has been found to be applicable for the dissociative chemisorption of H_2 , CH_4 , and H_2O .^{62–69} For CH_4 , the SVP model correctly predicted that the methane symmetric and asymmetric stretching modes are strong promoting modes with roughly equal efficacies, while the bending modes are less effective. The SVP predicted mode specificity is consistent with both experimental observations and reduced-dimensional quantum results.^{64–66} The mode specificity of D_2O has also been confirmed experimentally.⁶⁷ Furthermore, it was shown recently that the normal scaling behavior^{66,69} and surface lattice

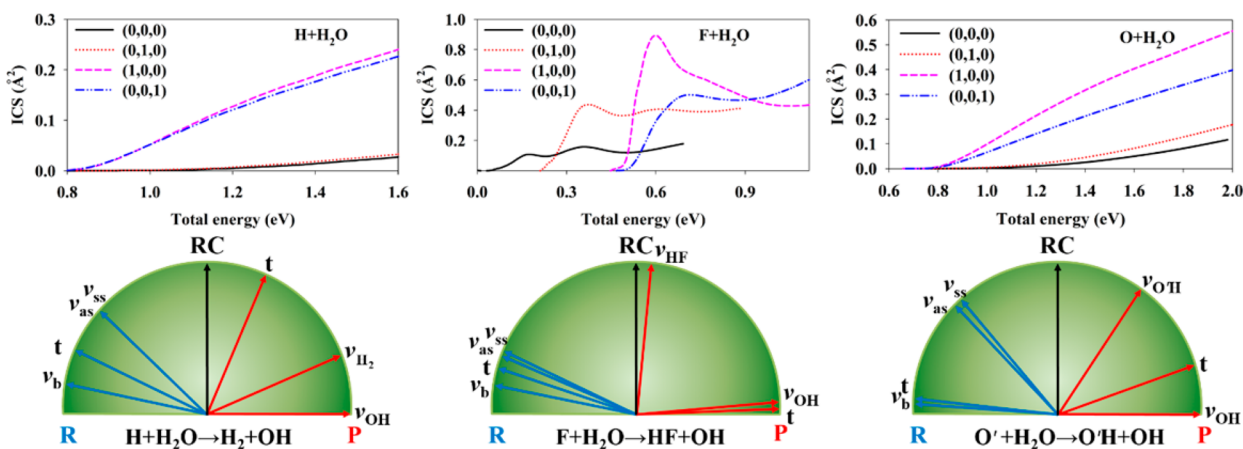


Figure 3. Calculated mode-specific total reaction integral cross sections for the $\text{X} + \text{H}_2\text{O} \rightarrow \text{HX} + \text{OH}$ ($\text{X} = \text{H}, \text{F}, \text{O}(^3\text{P})$) reactions and the SVP values for both reactant and product modes.³⁷

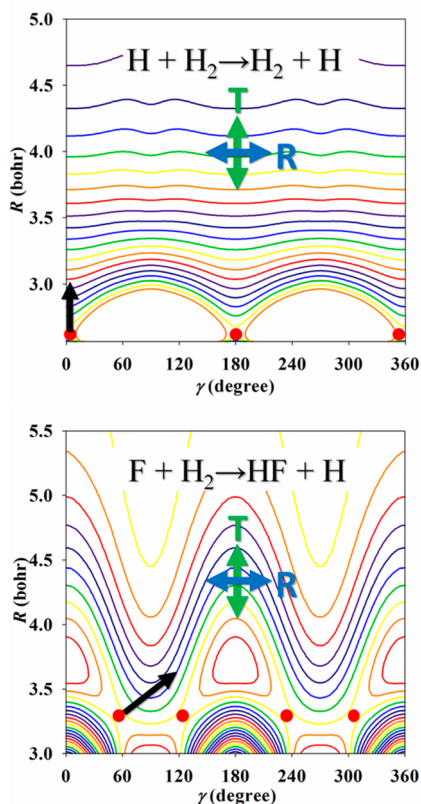


Figure 4. Contour plots of the PESs and alignment of the reactant rotational (R) and translational (T) vectors with the reaction coordinate at the transition state for the $X + H_2 \rightarrow HX + H$ ($X = H, F$) reactions.⁴⁸ The red dots denote the transition state.

effects⁶⁹ can also be examined with the SVP model. Apparently, the success of the SVP model can again be attributed to the time scale disparity. Although fast energy transfer and IVR are expected once the reactant reaches the surface, the internal energy deposited in a particular mode of the incident molecule does not flow to other modes sufficiently quickly before hitting the surface.⁷⁰

While Polanyi's rules do not explicitly apply to bond selectivity, the SVP model has been shown to predict bond selectivity in both gas phase^{37,47} and surface reactions.^{62,65} The excitation of a local mode vibration associated with the breaking bond strongly promotes the corresponding reaction channel, thanks to the strong coupling with the RC at the related transition state.

It is interesting to compare the SVP model with the vibrationally adiabatic model based on the reaction path Hamiltonian (RPH),⁷¹ which expresses the reaction system with N atoms in terms of the RC (s) and $3N - 7$ generalized normal modes along s . Within the adiabatic limit, potential energy curves can be constructed to connect reactant internal levels with product internal levels. It has been shown that when one reactant approaches the other, some vibrational modes soften in response to chemical forces near the transition state. As a result, adiabatic barriers for the excited vibrational states might be lowered relative to that of the ground vibrational state for the reactant.^{18,72–74} Taking the example of the $Cl + CH_4$ reaction again, the initial symmetric stretching mode of CH_4 softens near the transition state as it morphs into the proximal C–H vibration, eventually leading to the H transfer to Cl. The

lower frequency for this mode near the saddle point leads to a lowered adiabatic barrier, which explains its promotional effect. Similar mode softening is also found for the umbrella mode, also leading to some reactivity enhancement. On the other hand, the three degenerate asymmetric stretching modes of CH_4 change into three distal C–H vibrations, which are essentially spectators of the reaction in this adiabatic picture. Their frequencies stay roughly the same, resulting in essentially the same barriers as that of the ground vibrational state. The substantial enhancement of the asymmetric stretching excitation can only be explained by vibrational nonadiabaticity, which allows the system to hop onto other vibrational states with lower barriers.

It is apparent that the adiabatic picture described above represents the complementary case of the sudden limit. However, the fact that nonadiabatic transitions have to be invoked to explain the promotional effect of the CH_4 asymmetric stretching mode suggests that the adiabatic picture is less appropriate for mode specific processes. On the contrary, the SVP model predicts that both stretching modes of methane are of almost equal efficacy in promoting the reaction,⁴⁷ consistent with both theoretical and experimental evidence. The sudden and adiabatic models provide two limiting cases for all reactions, although mode specific reactions are most likely near the sudden limit because of the slow IVR rates in their reactants. Equivalently, there are reactions that follow more closely to the adiabatic picture.

By now, it is clear that the answer to the first question raised above is positive. In other words, a simple set of rules can indeed be found to predict mode specificity and bond selectivity in both gas phase and gas–surface reactions. However, what do these rules reveal in terms of fundamental principles governing these dynamical phenomena? To answer this question, it is helpful to point out that the SVP model is based on a transition-state property, namely, the RC vector at the saddle point. Hence, its success suggests that mode specificity and bond selectivity are essentially controlled by the transition state.³⁷ This is not an entirely surprising conclusion, since there has been ample supporting evidence. For example, Schatz and Ross showed some time ago that state-to-state reaction probabilities can be approximately recovered by Franck–Condon overlaps of the reactant and product inelastic scattering wave functions in the transition state region.⁷⁵ Similarly, Wang and Bowman used a Franck–Condon model to predict successfully the product state distribution of a bimolecular reaction from a transition-state wave function.⁷⁶ More recently, Gustafsson and Skodje demonstrated that reactive S-matrix elements can be approximately obtained by assembling the Franck–Condon overlaps between reactant or product and transition-state wave functions.⁷⁷ In addition, exact schemes have recently been proposed for the calculation of the S-matrix elements by propagating transition-state wave packets separately to both the reactant and product channels.^{78–81} Interestingly, this transition-state wave packet approach showed little energy flow in the decomposition of the activated complex, validating the sudden approximation.⁸² It is thus clear that the SVP model is deeply rooted in the transition-state concept, which accentuates the point that mode specificity is largely controlled by the saddle point of the reaction path. Practically, this realization is an important one, because the SVP values can be obtained directly from the *ab initio* determination of saddle point properties. Such capacity is of great value for

researchers who would like to study mode specificity in reactions that have no PESs available.

Finally, we would like to point out that as any simple empirical rules, the SVP model is no panacea. It is expected to fail when its underlying assumptions are violated. For example, if the IVR rate in the reactant is sufficiently fast, which is typical for large molecules with heavy atoms, the sudden approximation is not expected to hold. The model is also expected to falter if there is a deep prereaction complex that exerts strong stereodynamical forces on the reactants, particularly at low collision energies. Neither will the SVP model be applicable if the reaction is dominated by one or more stable reaction intermediates where IVR is strong, nor if the energy is significantly higher than the barrier since the transition state no longer controls the reaction. Since it is based on the normal mode picture, it can predict neither the energy dependence of mode specificity nor the efficacies of overtone and combination excitations. Finally, it is noted that predictions involving bending and rotational modes are not as reliable because of the much lower frequencies in the angular modes at the transition state.

To summarize, we have proposed a simple yet powerful model for predicting mode specificity and bond selectivity in gas phase and gas–surface reactions. This SVP model is based on the premise that the collision time is so fast that the reaction can be considered in the sudden limit. More importantly, it attributes the coupling of a reactant mode with the RC at the transition state to the alignment of the corresponding normal mode vectors. As a result, it is applicable to reactions involving polyatomic molecules. Despite its many limitations, the SVP model has been successfully applied to several reactions and is expected to shed further light on many others. A Fortran code of the SVP model based on frequency calculations in multiple quantum chemistry software packages, including Polyrate, Gaussian, Molpro, and VASP, is available at <http://www.unm.edu/~hguo/Research.html>.

AUTHOR INFORMATION

Corresponding Author

*Professor Hua Guo. Phone: 5052771716. Fax: 5052772609. E-mail: hguo@unm.edu.

Funding

We thank the National Science Foundation and the Basic Energy Science Program of Department of Energy for financial support.

Notes

The authors declare no competing financial interest.

Biographies

Hua Guo is Professor of Chemistry at Department of Chemistry and Chemical Biology, University of New Mexico. After his undergraduate and M.S. training in China, he went to the U.K. to study theoretical chemistry with Professor John Murrell, FRS, at Sussex University, receiving his D.Phil. degree in 1988. He spent two years at Northwestern University as a postdoctoral fellow with Professor George Schatz. His independent career started as Assistant Professor at University of Toledo in 1990, and he moved to University of New Mexico in 1998. His research interests include gas phase reaction dynamics, photochemistry, surface reactions, and catalysis, as well as mechanistic enzymology.

Bin Jiang is a Postdoctoral Fellow with Professor Hua Guo in Department of Chemistry and Chemical Biology, University of New Mexico. He received his Ph.D. at Nanjing University, China, in 2012 with Professor Daiqian Xie. He is currently interested in *ab initio* potential energy surfaces and quantum/classical dynamics of chemical reactions in gas phase or at the gas–surface interface.

REFERENCES

- (1) Crim, F. F. Vibrational state control of bimolecular reactions: Discovering and directing the chemistry. *Acc. Chem. Res.* **1999**, *32*, 877–884.
- (2) Crim, F. F. Chemical dynamics of vibrationally excited molecules: Controlling reactions in gases and on surfaces. *Proc. Natl. Acad. Sci. U.S.A.* **2008**, *105*, 12654–12661.
- (3) Zare, R. N. Laser control of chemical reactions. *Science* **1998**, *279*, 1875–1879.
- (4) Sinha, A.; Hsiao, M. C.; Crim, F. F. Controlling bimolecular reactions: Mode and bond selected reaction of water with hydrogen atoms. *J. Chem. Phys.* **1991**, *94*, 4928–4935.
- (5) Sinha, A.; Thoemke, J. D.; Crim, F. F. Controlling bimolecular reactions: Mode and bond selected reaction of water with translationally energetic chlorine atoms. *J. Chem. Phys.* **1992**, *96*, 372–376.
- (6) Simpson, W. R.; Rakitzis, T. P.; Kandel, S. A.; Orr-Ewing, A. J.; Zare, R. N. Reaction of Cl with vibrationally excited CH₄ and CHD₃ - State-to-state differential cross sections and steric effects for the HCl product. *J. Chem. Phys.* **1995**, *103*, 7313–7335.
- (7) Yoon, S.; Henton, S.; Zivkovic, A. N.; Crim, F. F. The relative reactivity of the stretch-bend combination vibrations of CH₄ in the Cl(²P_{3/2}) + CH₄ reaction. *J. Chem. Phys.* **2002**, *116*, 10744–10752.
- (8) Bechtel, H. A.; Camden, J. P.; Brown, D. J. A.; Zare, R. N. Comparing the dynamical effects of symmetric and antisymmetric stretch excitation of methane in the Cl+CH₄ reaction. *J. Chem. Phys.* **2004**, *120*, 5096–5103.
- (9) Camden, J. P.; Bechtel, H. A.; Brown, D. J. A.; Zare, R. N. Effects of C-H stretch excitation on the H+CH₄ reaction. *J. Chem. Phys.* **2005**, *123*, 134301.
- (10) Yan, S.; Wu, Y. T.; Zhang, B.; Yue, X.-F.; Liu, K. Do vibrational excitations of CHD₃ preferentially promote reactivity toward the chlorine atom? *Science* **2007**, *316*, 1723–1726.
- (11) Riedel, J.; Yan, S. N.; Liu, K. Mode specificity in reactions of Cl with CH₂ stretch-excited CH₂D₂($\nu_1, \nu_6 = 1$). *J. Phys. Chem. A* **2009**, *113*, 14270–14276.
- (12) Zhang, W.; Kawamata, H.; Liu, K. CH stretching excitation in the early barrier F + CHD₃ reaction Inhibits CH bond cleavage. *Science* **2009**, *325*, 303–306.
- (13) Wang, F.; Liu, K. Enlarging the reactive cone of acceptance by exciting the C-H bond in the O(³P) + CHD₃ reaction. *Chem. Sci.* **2010**, *1*, 126–133.
- (14) Kawamata, H.; Zhang, W. Q.; Liu, K. Imaging the effects of the antisymmetric stretch excitation of CH₄ in the reaction with F atom. *Faraday Discuss.* **2012**, *157*, 89–100.
- (15) Bronikowski, M. J.; Simpson, W. R.; Zare, R. N. Effect of reagent vibration on the H + HOD reaction: An example of bond-specific chemistry. *J. Phys. Chem.* **1993**, *97*, 2194–2203.
- (16) Pfeiffer, J. M.; Woods, E.; Metz, R. B.; Crim, F. F. Probing the new bond in the vibrationally controlled bimolecular reaction of O with HOD(4 ν_{OH}). *J. Chem. Phys.* **2000**, *113*, 7982–7987.
- (17) Kim, Z. H.; Bechtel, H. A.; Zare, R. N. Vibrational control in the reaction of methane with atomic chlorine. *J. Am. Chem. Soc.* **2001**, *123*, 12714–12715.
- (18) Yoon, S.; Holiday, R. J.; Crim, F. F. Control of bimolecular reactions: Bond-selected reaction of vibrationally excited CH₃D with Cl(²P_{3/2}). *J. Chem. Phys.* **2003**, *119*, 4755–4761.
- (19) Camden, J. P.; Bechtel, H. A.; Brown, D. J. A.; Zare, R. N. Comparing reactions of H and Cl with C-H stretch-excited CHD₃. *J. Chem. Phys.* **2006**, *124*, 034311.

- (20) Crim, F. F. Vibrationally mediated photodissociation: Exploring excited-state surfaces and controlling decomposition pathways. *Annu. Rev. Phys. Chem.* **1993**, *44*, 397–428.
- (21) Reid, S. A.; Reisler, H. Experimental studies of resonances in unimolecular decomposition. *Annu. Rev. Phys. Chem.* **1996**, *47*, 495–525.
- (22) Juurlink, L. B. F.; Killelea, D. R.; Utz, A. L. State-resolve probes of methane dissociation dynamics. *Prog. Surf. Sci.* **2009**, *84*, 69–134.
- (23) Beck, R. D.; Utz, A. L. In *Dynamics of Gas-Surface Interactions*; Muino, R. D., Busnengo, H. F., Eds.; Springer: Heidelberg, 2013.
- (24) Schatz, G. C.; Colton, M. C.; Grant, J. L. A quasiclassical trajectory study of the state-to-state dynamics of $\text{H} + \text{H}_2\text{O} \rightarrow \text{OH} + \text{H}_2$. *J. Phys. Chem.* **1984**, *88*, 2971–2977.
- (25) Zhang, D. H.; Light, J. C. A six-dimensional quantum study for atom-triatom reactions: The $\text{H} + \text{H}_2\text{O} \rightarrow \text{H}_2 + \text{OH}$ reaction. *J. Chem. Phys.* **1996**, *104*, 4544–4553.
- (26) Zhang, D. H.; Light, J. C. Mode specificity in the $\text{H} + \text{HOD}$ reaction: Full-dimensional quantum study. *J. Chem. Soc., Faraday Trans.* **1997**, *93*, 691–697.
- (27) Zhang, D. H.; Collins, M. A.; Lee, S.-Y. First-principles theory for the $\text{H} + \text{H}_2\text{O}$, D_2O reactions. *Science* **2000**, *290*, 961–963.
- (28) Yang, M.; Lee, S.-Y.; Zhang, D. H. Seven-dimensional quantum dynamics study of the $\text{O}(^3\text{P}) + \text{CH}_4$ reaction. *J. Chem. Phys.* **2007**, *126*, No. 064303.
- (29) Czakó, G.; Bowman, J. M. CH stretching excitation steers the F atom to the CD bond in the $\text{F} + \text{CHD}_3$ reaction. *J. Am. Chem. Soc.* **2009**, *131*, 17534–17535.
- (30) Czakó, G.; Shuai, Q. A.; Liu, K.; Bowman, J. M. Communication: Experimental and theoretical investigations of the effects of the reactant bending excitations in the $\text{F} + \text{CHD}_3$ reaction. *J. Chem. Phys.* **2010**, *133*, No. 131101.
- (31) Czakó, G.; Bowman, J. M. Dynamics of the reaction of methane with chlorine atom on an accurate potential energy surface. *Science* **2011**, *334*, 343–346.
- (32) Czakó, G.; Bowman, J. M. Dynamics of the $\text{O}(^3\text{P}) + \text{CHD}_3(\nu_{\text{CH}}=0,1)$ reactions on an accurate ab initio potential energy surface. *Proc. Natl. Acad. Sci. U.S.A.* **2012**, *109*, 7997–8001.
- (33) Liu, R.; Yang, M.; Czakó, G.; Bowman, J. M.; Li, J.; Guo, H. Mode selectivity for a “central” barrier reaction: Eight-dimensional quantum studies of the $\text{O}(^3\text{P}) + \text{CH}_4 \rightarrow \text{OH} + \text{CH}_3$ reaction on an ab initio potential energy surface. *J. Phys. Chem. Lett.* **2012**, *3*, 3776–3780.
- (34) Zhang, Z.; Zhou, Y.; Zhang, D. H.; Czakó, G.; Bowman, J. M. Theoretical study of the validity of the Polanyi rules for the late-barrier $\text{Cl} + \text{CHD}_3$ reaction. *J. Phys. Chem. Lett.* **2012**, *3*, 3416–3419.
- (35) Czakó, G.; Liu, R.; Yang, M.; Bowman, J. M.; Guo, H. Quasiclassical trajectory studies of the $\text{O}(^3\text{P}) + \text{CX}_4(\nu_k = 0, 1) \rightarrow \text{OX}(\nu) + \text{CX}_3(n_1n_2n_3n_4)$ [$\text{X} = \text{H}$ and D] reactions on an ab initio potential energy surface. *J. Phys. Chem. A* **2013**, *117*, 6409–6420.
- (36) Fu, B.; Zhang, D. H. Mode specificity in the $\text{H} + \text{H}_2\text{O} \rightarrow \text{H}_2 + \text{OH}$ reaction: A full-dimensional quantum dynamics study. *J. Chem. Phys.* **2013**, *138*, No. 184308.
- (37) Jiang, B.; Guo, H. Control of mode/bond selectivity and product energy disposal by the transition state: The $\text{X} + \text{H}_2\text{O}$ ($\text{X} = \text{H}$, F , $\text{O}(^3\text{P})$, and Cl) reactions. *J. Am. Chem. Soc.* **2013**, *135*, 15251–15256.
- (38) Czakó, G.; Bowman, J. M. Reaction dynamics of methane with F , O , Cl , and Br on ab initio potential energy surfaces. *J. Phys. Chem. A* **2014**, *118*, 2839–2864.
- (39) Polanyi, J. C. Concepts in reaction dynamics. *Acc. Chem. Res.* **1972**, *5*, 161–168.
- (40) Wang, F.; Lin, J.-S.; Cheng, Y.; Liu, K. Vibrational enhancement factor of the $\text{Cl} + \text{CHD}_3(\nu_1=1)$ reaction: Rotational-probe effects. *J. Phys. Chem. Lett.* **2013**, *4*, 323–327.
- (41) Li, J.; Jiang, B.; Guo, H. Reactant vibrational excitations of reactant are more effective than translational energy in promoting an early-barrier reaction $\text{F} + \text{H}_2\text{O} \rightarrow \text{HF} + \text{OH}$. *J. Am. Chem. Soc.* **2013**, *135*, 982–985.
- (42) Nesbitt, D. J.; Field, R. W. Vibrational energy flow in highly excited molecules: Role of intramolecular vibrational redistribution. *J. Phys. Chem.* **1996**, *100*, 12735–12756.
- (43) Jiang, B.; Guo, H. Relative efficacy of vibrational vs. translational excitation in promoting atom-diatom reactivity: Rigorous examination of Polanyi's rules and proposition of sudden vector projection (SVP) model. *J. Chem. Phys.* **2013**, *138*, No. 234104.
- (44) Wilson, E. B.; Decius, J. C.; Cross, P. C. *Molecular Vibrations*; Dover: New York, 1955.
- (45) Corchado, J. C.; Chuang, Y.-Y.; Fast, P. L.; Hu, W.-P.; Liu, Y.-P.; Lynch, G. C.; Nguyen, K. A.; Jackels, C. F.; Fernandez Ramos, A.; Ellingson, B. A.; Lynch, B. J.; Zheng, J.; Melissas, V. S.; Villà, J.; Rossi, I.; Coitiño, E. L.; Pu, J.; Albu, T. V.; Steckler, R.; Garrett, B. C.; Isaacson, A. D.; Truhlar, D. G. POLYRATE, version 9.7, University of Minnesota, Minneapolis, 2007.
- (46) Frisch, M. J.; Trucks, G. W.; Schlegel, H. B.; Scuseria, G. E.; Robb, M. A.; Cheeseman, J. R.; Scalmani, G.; Barone, V.; Mennucci, B.; Petersson, G. A.; Nakatsuji, H.; Caricato, M.; Li, X.; Hratchian, H. P.; Izmaylov, A. F.; Bloino, J.; Zheng, G.; Sonnenberg, J. L.; Hada, M.; Ehara, M.; Toyota, K.; Fukuda, R.; Hasegawa, J.; Ishida, M.; Nakajima, T.; Honda, Y.; Kitao, O.; Nakai, H.; Vreven, T.; Montgomery, J. A., Jr.; Peralta, J. E.; Ogliaro, F.; Bearpark, M.; Heyd, J. J.; Brothers, E.; Kudin, K. N.; Staroverov, V. N.; Kobayashi, R.; Normand, J.; Raghavachari, K.; Rendell, A.; Burant, J. C.; Iyengar, S. S.; Tomasi, J.; Cossi, M.; Rega, N.; Millam, J. M.; Klene, M.; Knox, J. E.; Cross, J. B.; Bakken, V.; Adamo, C.; Jaramillo, J.; Gomperts, R.; Stratmann, R. E.; Yazyev, O.; Austin, A. J.; Cammi, R.; Pomelli, C.; Ochterski, J. W.; Martin, R. L.; Morokuma, K.; Zakrzewski, V. G.; Voth, G. A.; Salvador, P.; Dannenberg, J. J.; Dapprich, S.; Daniels, A. D.; Farkas, O.; Foresman, J. B.; Ortiz, J. V.; Cioslowski, J.; Fox, D. J. *Gaussian 09*, revision C.01; Gaussian, Inc.: Wallingford, CT, 2009.
- (47) Jiang, B.; Guo, H. Mode specificity, bond selectivity, and product energy disposal in $\text{X} + \text{CH}_4/\text{CHD}_3$ ($\text{X} = \text{H}$, F , $\text{O}(^3\text{P})$, Cl , and OH) hydrogen abstraction reaction: Perspective from sudden vector projection model. *J. Chin. Chem. Soc.* **2014**, *61*, 841–959.
- (48) Jiang, B.; Li, J.; Guo, H. Effects of reactant rotational excitation on reactivity: Perspectives from the sudden limit. *J. Chem. Phys.* **2014**, *140*, No. 034112.
- (49) Li, A.; Guo, H.; Sun, Z. G.; Klos, J.; Alexander, M. H. State-to-state quantum dynamics of the $\text{F} + \text{HCl}(\nu_1=0, j_1=0) \rightarrow \text{HF}(\nu_b, j_b) + \text{Cl}$ reaction on the ground state potential energy surface. *Phys. Chem. Chem. Phys.* **2013**, *15*, 15347–15355.
- (50) Li, J.; Guo, H. Quasi-classical trajectory study of the $\text{F} + \text{H}_2\text{O} \rightarrow \text{HF} + \text{OH}$ reaction: Influence of barrier height, reactant rotational excitation, and isotopic substitution. *Chin. J. Chem. Phys.* **2013**, *26*, 627–634.
- (51) Song, H.; Li, J.; Guo, H. Mode specificity in the $\text{HF} + \text{OH} \rightarrow \text{F} + \text{H}_2\text{O}$ reaction. *J. Chem. Phys.* **2014**, *141*, No. 164316.
- (52) Li, J.; Guo, H. A nine-dimensional global potential energy surface for $\text{NH}_4(\text{X}^2\text{A}_1)$ and kinetics studies on the $\text{H} + \text{NH}_3 \leftrightarrow \text{H}_2 + \text{NH}_2$ reaction. *Phys. Chem. Chem. Phys.* **2014**, *16*, 6753–6763.
- (53) Song, H.; Li, J.; Yang, M.; Lu, Y.; Guo, H. Nine-dimensional quantum dynamics study of the $\text{H}_2 + \text{NH}_2 \rightarrow \text{H} + \text{NH}_3$ reaction: A rigorous test of the sudden vector projection model. *Phys. Chem. Chem. Phys.* **2014**, *16*, 17770–17776.
- (54) Li, A.; Guo, H. A nine-dimensional ab initio global potential energy surface for the $\text{H}_2\text{O}^+ + \text{H}_2 \rightarrow \text{H}_3\text{O}^+ + \text{H}$ reaction. *J. Chem. Phys.* **2014**, *140*, No. 224313.
- (55) Liu, R.; Wang, F.; Jiang, B.; Czakó, G.; Yang, M.; Liu, K.; Guo, H. Rotational mode specificity in the $\text{Cl} + \text{CHD}_3 \rightarrow \text{HCl} + \text{CD}_3$ reaction. *J. Chem. Phys.* **2014**, *141*, No. 074310.
- (56) Song, H.; Li, J.; Jiang, B.; Yang, M.; Lu, Y.; Guo, H. Effects of reactant rotation on the dynamics of the $\text{OH} + \text{CH}_4 \rightarrow \text{H}_2\text{O} + \text{CH}_3$ reaction: A six-dimensional study. *J. Chem. Phys.* **2014**, *140*, No. 084307.
- (57) Li, J.; Guo, H. Mode specificity in unimolecular reactions, insights from the sudden vector projection model. *J. Phys. Chem. A* **2014**, *118*, 2419–2425.

- (58) Wang, J.; Li, J.; Ma, J.; Guo, H. Full-dimensional characterization of photoelectron spectra of HOCO^- and DOCO^- and tunneling facilitated decay of HOCO prepared by anion photodetachment. *J. Chem. Phys.* **2014**, *140*, No. 184314.
- (59) Wang, Y.; Bowman, J. M. Mode-specific tunneling using the Q_{im} path: Theory and an application to full-dimensional malonaldehyde. *J. Chem. Phys.* **2013**, *139*, No. 154303.
- (60) Wang, X.; Bowman, J. M. Mode-specific tunneling in the unimolecular dissociation of cis- HOCO to $\text{H} + \text{CO}_2$. *J. Phys. Chem. A* **2014**, *118*, 684–689.
- (61) Homayoon, Z.; Bowman, J. M.; Evangelista, F. A. Calculations of mode-specific tunneling of double-hydrogen transfer in porphycene agree with and illuminate experiment. *J. Phys. Chem. Lett.* **2014**, *5*, 2723–2727.
- (62) Jiang, B.; Xie, D.; Guo, H. Vibrationally mediated bond selective dissociative chemisorption of HOD on $\text{Cu}(111)$. *Chem. Sci.* **2013**, *4*, 503–508.
- (63) Jiang, B.; Ren, X.; Xie, D.; Guo, H. Enhancing dissociative chemisorption of H_2O on $\text{Cu}(111)$ via vibrational excitation. *Proc. Natl. Acad. Sci. U.S.A.* **2012**, *109*, 10224–10227.
- (64) Jiang, B.; Liu, R.; Li, J.; Xie, D.; Yang, M.; Guo, H. Mode selectivity in methane dissociative chemisorption on $\text{Ni}(111)$. *Chem. Sci.* **2013**, *4*, 3249–3254.
- (65) Jiang, B.; Guo, H. Mode and bond selectivities in methane dissociative chemisorption: Quasi-classical trajectory studies on twelve-dimensional potential energy surface. *J. Phys. Chem. C* **2013**, *117*, 16127–16135.
- (66) Jackson, B.; Nattino, F.; Kroes, G.-J. Dissociative chemisorption of methane on metal surfaces: Tests of dynamical assumptions using quantum models and ab initio molecular dynamics. *J. Chem. Phys.* **2014**, *141*, No. 054102.
- (67) Hundt, P. M.; Jiang, B.; van Reijzen, M.; Guo, H.; Beck, R. D. Vibrationally promoted dissociation of water on $\text{Ni}(111)$. *Science* **2014**, *344*, 504–507.
- (68) Jiang, B.; Guo, H. Six-dimensional quantum dynamics for dissociative chemisorption of H_2 and D_2 on $\text{Ag}(111)$ on a permutation invariant potential energy surface. *Phys. Chem. Chem. Phys.* **2014**, *16*, 24704–24715.
- (69) Jiang, B.; Guo, H. Prediction of mode specificity, bond selectivity, normal scaling, and surface lattice effects in water dissociative chemisorption on several metal surfaces using the sudden vector projection model. *J. Phys. Chem. C* **2014**, DOI: 10.1021/jp5090839.
- (70) Killelea, D. R.; Utz, A. L. On the origin of mode- and bond-selectivity in vibrationally mediated reactions on surfaces. *Phys. Chem. Chem. Phys.* **2013**, *15*, 20545–20554.
- (71) Miller, W. H.; Handy, N. C.; Adams, J. E. Reaction path Hamiltonian for polyatomic molecules. *J. Chem. Phys.* **1980**, *72*, 99–112.
- (72) Duncan, W. T.; Truong, T. N. Thermal and vibrational-state selected rates of the $\text{CH}_4 + \text{Cl} \leftrightarrow \text{HCl} + \text{CH}_3$ reaction. *J. Chem. Phys.* **1995**, *103*, 9642–9652.
- (73) Halonen, L.; Bernasek, S. L.; Nesbitt, D. J. Reactivity of vibrationally excited methane on nickel surfaces. *J. Chem. Phys.* **2001**, *115*, 5611–5620.
- (74) Yan, S.; Wu, Y.-T.; Liu, K. Tracking the energy flow along the reaction path. *Proc. Natl. Acad. Sci. U.S.A.* **2008**, *105*, 12667–12672.
- (75) Schatz, G. C.; Ross, J. Franck-Condon factors in studies of dynamics of chemical reactions. I. General theory, application to collinear atom-diatom reactions. *J. Chem. Phys.* **1977**, *66*, 1021–1036.
- (76) Wang, D.; Bowman, J. M. An adiabatic-bend Franck-Condon model for final rotational distributions in the $\text{H} + \text{H}_2\text{O}$ and $\text{H} + \text{D}_2\text{O}$ reactions. *Chem. Phys. Lett.* **1993**, *207*, 227–235.
- (77) Gustafsson, M.; Skodje, R. T. The state-to-state model for direct chemical reactions: Application to $\text{D} + \text{H}_2 \rightarrow \text{HD} + \text{H}$. *J. Chem. Phys.* **2006**, *124*, No. 144311.
- (78) Welsch, R.; Huarte-Larrañaga, F.; Manthe, U. State-to-state reaction probabilities within the quantum transition state framework. *J. Chem. Phys.* **2012**, *136*, No. 064117.
- (79) Manthe, U.; Welsch, R. Correlation functions for fully or partially state-resolved reactive scattering calculations. *J. Chem. Phys.* **2014**, *140*, No. 244113.
- (80) Zhao, B.; Sun, Z.; Guo, H. Calculation of state-to-state differential and integral cross sections for atom-diatom reactions with transition-state wave packets. *J. Chem. Phys.* **2014**, *140*, No. 234110.
- (81) Zhao, B.; Sun, Z.; Guo, H. Calculation of the state-to-state S-matrix for tetra-atomic reactions with transition-state wave packets: $\text{H}_2/\text{D}_2 + \text{OH} \rightarrow \text{H}/\text{D} + \text{H}_2\text{O}/\text{HOD}$. *J. Chem. Phys.* **2014**, *141*, No. 154112.
- (82) Welsch, R.; Manthe, U. Communication: Ro-vibrational control of chemical reactivity in $\text{H} + \text{CH}_4 \rightarrow \text{H}_2 + \text{CH}_3$: Full-dimensional quantum dynamics calculations and a sudden model. *J. Chem. Phys.* **2014**, *141*, No. 051102.